CHEMISTRY OF MATERIALS
Article

Chem. Mater. **2010,** *22,* 5521–5527 5521
DOI:10.1021/cm101503y

Enhanced Figure-of-Merit in Se-Doped p-Type $AgSbTe_2$ Thermoelectric Compound

Baoli Du,[†,‡] Han Li,[†] Jingjing Xu,[†] Xinfeng Tang,*[,†] and Ctirad Uher[§]

[†]*State Key Laboratory of Advanced Technology for Materials Synthesis and Processing, Wuhan University of Technology, Wuhan 430070, China,* [‡]*School of Physics and Chemistry, Henan Polytechnic University, Jiaozuo 454000, China, and* [§]*Department of Physics, University of Michigan, Ann Arbor, Michigan 48109*

Received May 28, 2010. Revised Manuscript Received August 23, 2010

Polycrystalline, sintered samples of p-type $AgSbSe_xTe_{2-x}$ ($x = 0-0.04$) were prepared from high purity elements by a melt-quench technique followed by spark plasma sintering. X-ray diffraction and differential scanning calorimetry thermal analysis indicate that a small amount of Se doping ($x \geq 0.02$) can effectively inhibit the emergence of the Ag_2Te and $Ag_{0.35}Sb_{0.09}Te_{0.56}$ impurity phases. Therefore, samples with $x \geq 0.02$ form a homogeneous single-phase solid solution and in the temperature range 400−700 K have considerably larger electrical conductivity compared with that of samples with $x = 0$ and $x = 0.01$. Combined with a low lattice thermal conductivity, samples with $x \geq 0.02$ have a higher figure of merit ZT that reaches values of 1.37 at 565 K, representing a 26% enhancement with respect to an undoped $AgSbTe_2$ at the same temperature. The results indicate that doping with Se is an effective way to enhance the thermoelectric performance of p-type $AgSbTe_2$.

Introduction

Thermoelectricity has long been recognized as a promising transformative energy conversion technology because of its ability to convert heat directly into electricity based on the Seebeck effect.[1] Compared with other types of energy conversion technologies, thermoelectricity has distinct advantages such as simple equipment, no moving parts, no environmentally harmful fluids, and exceptionally high reliability. The efficiency of a thermoelectric (TE) material is judged by a parameter called thermoelectric figure of merit that is defined as: $ZT = \alpha^2\sigma T/\kappa$, where T is the absolute temperature and α, σ, and κ, are the Seebeck coefficient and electrical and thermal conductivity of the material, respectively. From this, it is clear that a large α and σ is desirable along with a small κ. Meanwhile, in order to achieve reliable performance, thermoelectric materials must be thermodynamically stable and mechanically robust. Currently, the development of medium-temperature bulk TE materials (for solar thermal energy conversion and industrial waste heat recovery) is being intensively pursued worldwide.[2]

In recent years, the $AgSbTe_2$ compound has been repeatedly studied as a prospective p-type TE material for the use in the temperature range $T = 400-700$ K.[3−7] Because of the complexity of ordering of Ag/Sb on the face-centered lattice, the electronic properties of the $AgSbTe_2$ compound are quite intriguing and show anomalies.[5] Diffuse reflectance measurements[5] give a band gap of about 0.35 eV, whereas the electrical conductivity suggests a strongly degenerate behavior.[8] According to studies on atomic ordering and gap formation in Ag−Sb-based ternary chalcogenides, it was suggested that the anomalous electronic properties of $AgSbTe_2$ can be understood in terms of a small intrinsic band gap and shallow impurity states.[9] Electronic, optical, and lattice vibrational properties of $AgSbTe_2$ were investigated by highly refined first-principles calculations of its ground state with GGA and the excited-state properties by the screened exchange LDA method.[10] Results indicate that the Ag/Sb disorder can reduce the lattice thermal conductivity of $AgSbTe_2$ to its minimum possible value by umklapp and normal intrinsic phonon−phonon scattering processes without any significant reduction in the electrical conductivity. The flat valence band maximum and multipeak valence band structure is expected to result in a large positive Seebeck coefficient. Low thermal conductivity and large Seebeck coefficient make the $AgSbTe_2$ compound a very promising candidate for high efficiency p-type TE applications.

Although $AgSbTe_2$ has many advantages as a TE material, its thermodynamic stability is a controversial issue.[7] Based on

*Corresponding author. E-mail: tangxf@whut.edu.cn.

(1) Rowe, D. M. *Thermoelectrics Handbook: Macro to Nano*; CRC/Taylor & Francis: Boca Raton, FL, 2006.
(2) Xie, M.; Gruen, D. M. *J. Phys. Chem. B* **2010**No. 10.1021/jp9117387.
(3) Wang, H.; Li., J; Zhou, M.; Sui, T. *Appl. Phys. Lett.* **2008**, *93*, 202106.
(4) Jovovic, V.; Heremans, J. P. *Phys. Rev. B* **2008**, *77*, 245204.
(5) Lin-Hui, Y.; Khang, H.; Freeman, A. J.; Mahanti, S. D.; Jian, H.; Tritt, M. T.; Kanatzidis, M. G. *Phys. Rev. B* **2008**, *77*, 245203.
(6) Morelli, D. T.; Jovovic, V.; Heremans, J. P. *Phys. Rev. Lett.* **2008**, *101*, 035901.
(7) Wojciechowski, K. T.; Schmidt, M. *Phys. Rev. B* **2009**, *79*, 184202.
(8) Zhang, S. N.; Zhu, T. J.; Yang, S. H.; Yu, C.; Zhao, X. B. *Acta Mater.* **2010**, *58*, 4160–4169.
(9) Hoang, K.; Mahanti, S. D.; Salvador, J. R.; Kanatzidis, M. G. *Phys. Rev. Lett.* **2007**, *99*, 156403.
(10) Barabash, S. V.; Ozolins, V.; Wolverton, C. *Phys. Rev. Lett.* **2008**, *101*, 155704.

Published on Web 09/08/2010

the $Sb_2Te_3-Ag_2Te$ pseudobinary phase diagram,[11] it has been concluded that the cubic $AgSbTe_2$ compound only exists at high temperatures and is unstable and decomposes to Ag_2Te and Sb_2Te_3 below 633 K. Extensive elaborations on the $Sb_2Te_3-Ag_2Te$ and $Sb_2Te_3-Ag_2Te-Te$ phase diagrams confirm that a thermodynamically stable compound with the stoichiometric composition of $AgSbTe_2$ is, in fact, nonexistent.[12] It has been shown that in the temperature range from 300 to 817 K, the closest stable intermediate compound with a cubic $AgSbTe_2$ structure has the actual chemical composition of $Ag_{19}Sb_{29}Te_{52}$ (42−44 at % of Ag_2Te, close to $AgSbTe_2$).[13]

Many researchers noted that $AgSbTe_2$ samples, prepared by standard conditions such as melting and slow-cooling (MC),[7] zone melting (ZM),[14] mechanical alloying (MA),[3] sonochemical method,[15] hot pressing,[8] as well as by high-pressure and high-temperature (HPHT) techniques,[16] contain a small amount of precipitated Ag_2Te, $Ag_{0.35}Sb_{0.09}Te_{0.56}$, or other undesirable impurities. Because of the *n*-type conduction and structural phase transition[17] at 425 K, Ag_2Te impurity may have a negative impact on TE performance and mechanical properties. Thus, suppressing the formation of impurities is critical to optimizing the mechanical and TE properties. However, a recipe on how to do it effectively has not yet been reported on.

Unlike $AgSbTe_2$, the cubic $AgSbSe_2$ compound has a stoichiometric composition and is thermodynamically stable below its melting point. Electronic structure calculations[9] indicate that as one goes from Te to Se, the indirect band gap moves from negative to positive value, i.e., the compound changes from a semimetal to a semiconductor. Hence, doping with Se can effectively alleviate the impact of minority carriers on the transport properties. Wojciechowski et al.[7] synthesized $AgSbTe_2-AgSbSe_2$ pseudobinary system by the traditional MC method. However, X-ray diffraction (XRD) and differential scanning calorimetry (DSC) revealed that samples with Se at % ≤ 50 are inhomogeneous multiphase materials that show an endothermic peak assigned to the melting point of an eutectic with the nominal composition of $Ag_{0.35}Sb_{0.09}Te_{0.56}$ at 633 K.[13] Therefore, further research should focus on suppressing the formation of impurity phases and improving the TE performance by optimizing the preparation conditions and adjusting the content of Se.

In this study, bulk polycrystalline $AgSbSe_xTe_{2-x}$ (x = 0−0.04) compounds were prepared by the melt-quench spark plasma sintering (SPS) nonequilibrium route. The influence of Se doping on the thermodynamic properties, microstructure, and TE transport behavior is investigated systematically.

(11) Petzow, G.; Effenberg, G. *Ternary Alloys* **1988**, *2*, 554.
(12) Ayralmarin, R. M.; Brun, G.; Maurin, M.; Tedenac, J. C. *Eur. J. Solid State Inorg. Chem.* **1990**, *27*, 747–757.
(13) Marin-Ayral, R.; Legendre, B.; Brun, G.; Liautard, B.; Tedenac, J. *Thermochim. Acta* **1988**, *131*, 37–45.
(14) Wolfe, R.; Wernick, J.; Haszko, S. *J. Appl. Phys.* **1960**, *31*, 1959–1964.
(15) Xu, J.; Li, H.; Du, B.; Tang, X.; Zhang, Q.; Uher, C. *J. Mater. Chem.* **2010**, *20*, 6138–6143.
(16) Ma, H.; Su, T.; Zhu, P.; Guo, J.; Jia, X. *J. Alloys Compd.* **2008**, *454*, 415–418.
(17) Ragimov, S. S.; Aliev, S. A. *Inorg. Mater.* **2007**, *43*, 1184–1186.

Table 1. Some Room-Temperature Structural and Transport Parameters for $AgSbSe_xTe_{2-x}$ (x = 0−0.04) Samples

	x = 0	x = 0.01	x = 0.02	x = 0.04
density (g/cm^3)	7.033	7.002	7.001	7.000
relative density (%)	98.3	97.8	97.8	97.8
lattice parameter (Å)[a]	6.077(2)	6.076(6)	6.074(2)	6.071(4)
$R_H \times 10^{-8}$m^3 C^{1-}	39.84	−4.848	−5.133	−2.095
$N \times 10^{19}$ cm^{-3}	1.57			

[a] The lattice parameters are calculated by Rietveld refinement.

Experimental Section

Polycrystalline $AgSbSe_xTe_{2-x}$ (x = 0−0.04) samples were prepared by melt-quench-SPS. High-purity starting elements of Ag (99.995%, filament), Sb (99.9999%, shot), Te (99.999%, shot), and Se (99.95%, shot) were heated in carbon-coated fused silica tubes under a vacuum for 10 h, cooled to 823 K slowly, and then quenched in saturated brine. The obtained ingots were pulverized to powder, loaded into a graphite die, and sintered by SPS to form dense polycrystalline bulk materials. The sintering process was performed at 723 K for 5 min under the pressure of 35 MPa. Relative densities of all samples were greater than 97.5% (Table 1).

The phases of the samples were determined by XRD (X'Pert PRO-PANalytical, CuKa) and DSC, (TA, Q20, heating rate 30 K min^{-1} and sample mass 20 mg). The microstructure was investigated by field emission scanning electron microscopy (FESEM, Hitachi, S-4800) with energy dispersive X-ray spectroscopy (EDS). Electrical conductivity σ and Seebeck coefficient α were measured simultaneously by the standard four-probe methods in a He atmosphere (Sinkuriko: ZEM-1). Thermal conductivity κ was calculated using the equation $\kappa = \lambda C_p d$ from the thermal diffusivity λ obtained by a flash diffusivity method (LFA 457, Netzsch), specific heat C_p determined by a differential scanning calorimetry method (Q20, TA), and the density d obtained by the Archimedes method.

Results and Discussion

Phase Composition and Thermodynamic Property. Table 1 summarizes some of the structural and transport parameters obtained on $AgSbSe_xTe_{2-x}$ (x = 0−0.04). Because of the smaller covalent radius of Se (1.16 Å) in comparison to Te (1.36 Å), the lattice parameter decreases with the increasing content of Se. The linear dependence of the lattice parameter versus x indicates that Se is substituting Te in the crystal lattice.

Figure 1 shows XRD patterns of the $AgSbSe_xTe_{2-x}$ (x = 0−0.04) samples. All diffractions of the matrix phase can be indexed into the face-centered-cubic (fcc) $AgSbTe_2$ structure (JCPDS Card No. 15−0540). For sample with x = 0 (and to a lesser extent sample x = 0.01), weak diffraction peaks due to the Ag_2Te impurity that are often reported in the literature[3,7] are detected. This indicates that the x = 0 sample consists of the major phase $AgSbTe_2$ and the precipitated Ag_2Te. This is consistent with the phase diagram investigated by Marin et al.[13] in which the Ag_2Te ratio of the single-phase region ranges from 42 to 44 mol %, and changes with thermal history. However, as the substitution of Se for Te increases from x = 0 to x = 0.04, the weak diffraction peaks due to impurity become weaker and disappear altogether in the

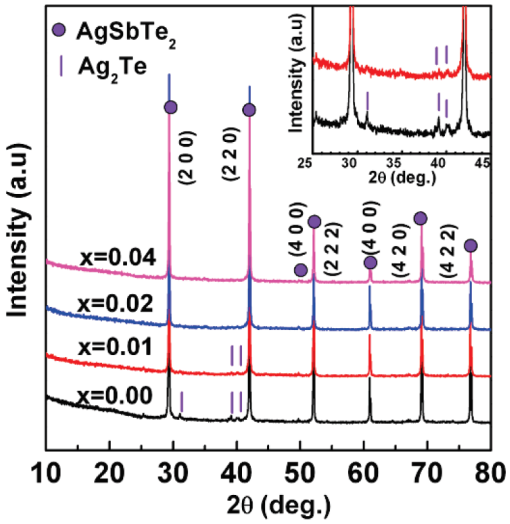

Figure 1. XRD patterns of $AgSbSe_xTe_{2-x}$ ($x = 0-0.04$) samples after SPS. The patterns from 2θ 35.5−44.5° for $x = 0$, 0.01 samples are magnified in the inset to show the precipitated Ag_2Te.

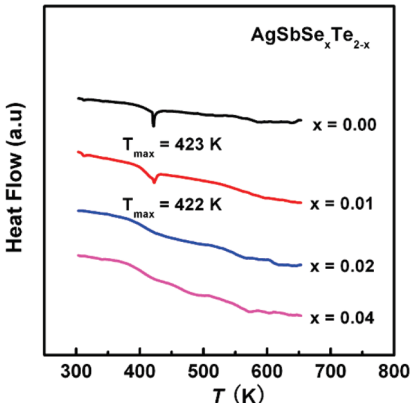

Figure 2. DSC curves of $AgSbSe_xTe_{2-x}$ ($x = 0-0.04$) samples.

background (shown in the inset of Figure 1). It suggests that, upon substituting Te with Se, the tendency to form impurity phases in $AgSbTe_2$ is suppressed.

To determine the phase composition of the obtained samples accurately, the DSC heat flow curves were measured and are plotted in Figure 2. We note the presence of an endothermic peak that appears in $AgSbTe_2$ and the sample with the lowest Se content ($AgSbSe_{0.01}Te_{1.99}$) around 425 K. We associate this peak with the $\alpha-\beta$ structural transition in Ag_2Te.[17] As x varies from 0 to 0.01, the area of the peak decreases. For samples with $x \geq 0.02$, the endothermic peak vanishes completely. Therefore, on the basis of the XRD and DSC analyses, we conclude that samples with $x = 0$ and $x = 0.01$ contain tiny amounts of Ag_2Te impurity, whereas samples with $x \geq 0.02$ are homogeneous single-phase solid solutions. We also note that the DSC analysis of all specimens examined in this research does not reveal any endothermic peak assigned to the melting point of a eutectic with the nominal composition $Ag_{0.35}Sb_{0.09}Te_{0.56}$ at 633 K as reported previously in refs 7 and 8. This indicates that a small amount of Se doping ($x \geq 0.02$) can inhibit the emergence of the Ag_2Te and $Ag_{0.35}Sb_{0.09}Te_{0.56}$ impurity phases quite effectively.

Images a and b in Figure 3 display the backscattered electron image (BSEI) and secondary electron image (SEI) of a polished $AgSbTe_2$ sample. The Widmanstätten pattern with ~1 μm flake-shaped precipitates is observed in this specimen. To determine the elemental component of the precipitates and the matrix, X-ray mapping is performed on the polished surface of the SPSed $AgSbTe_2$ sample, see Figure 3c−e. From the X-ray maps of Ag and Sb, we surmise that the Widmanstätten precipitates are Ag-rich and Sb-poor. Moreover, Widmanstätten precipitates regions are exactly consistent with the Ag-rich and Sb-poor regions in both position and shape. Figure 3f

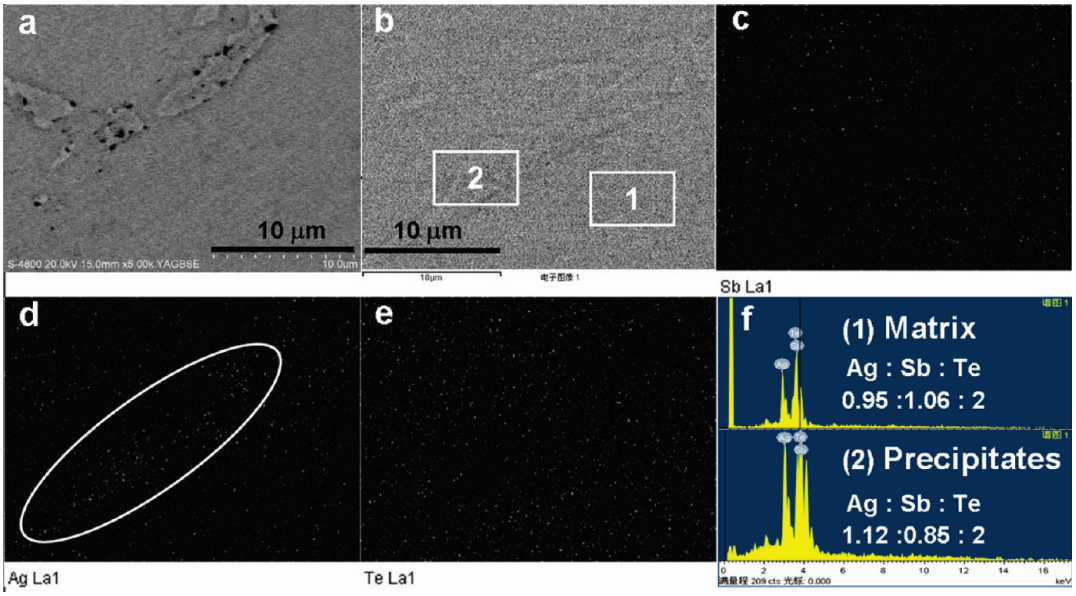

Figure 3. (a) Backscattered electron image (BSEI), (b) secondary electron image (SEI), (c−e) elemental distribution (ED) and (f) EDS results (1 matrix; 2 precipitates) for the $AgSbTe_2$ sample. The ED maps are on the same scale as SEI.

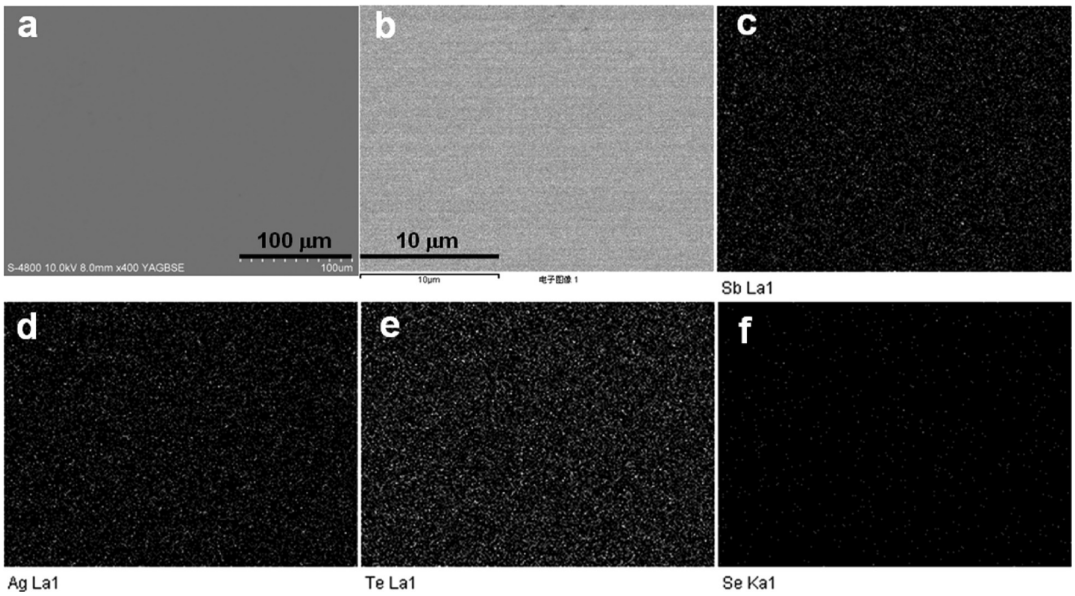

Figure 4. (a) Backscattered electron image (BSEI), (b) secondary electron image, and (c−f) elemental distribution (ED) for the $AgSbSe_{0.02}Te_{1.98}$ sample.

displays results of EDS which show the composition of the Widmanstätten precipitates and the surrounding matrix. The data confirm that the composition of Widmanstätten precipitates is Ag-rich and Sb-poor (the results are only of qualitative nature because the size of Widmanstätten precipitates is small and the composition is easily influenced by the surrounding matrix). The presence of Ag-rich and Sb-poor Widmanstätten precipitates likely indicates that the homogeneity range of the matrix is shifted toward the Sb-rich composition as was stated in ref 13. As shown in Figure 3f, the atomic ratio between Ag, Sb, and Te equals 0.95:1.06:2 in the matrix, seriously deviating from the nominal composition. From the pseudobinary phase diagram and the above results of XRD, DSC, and EDS, we conclude that the $AgSbTe_2$ sample is not homogeneous but rather composed of the Sb-rich matrix and a small amount of Ag_2Te impurity. The impact of the Ag_2Te impurity on TE properties will be discussed later on.

Contrasting the data in Figure 3 for the undoped $AgSbTe_2$, Figure 4 displays (a) BSEI, (b) SEI, and (c−f) X-ray maps of Ag, Sb, Te, and Se collected on the polished sample of $AgSbSe_{0.02}Te_{1.98}$. The BSEI and elemental maps are uniform with no notable darker and brighter regions. This indicates that there is no segregation of any elements and that they are distributed homogeneously in the matrix. Combining the above analysis, it demonstrates that small additives of Se can shift the composition of the homogeneity range from Sb-rich toward the ideal ratio Ag:Sb:(Te, Se) = 1:1:2. Thus, a small amount of Te substituted by Se ($x \geq 0.02$) is an effective way to obtain a single-phase $AgSbTe_2$ compound by suppressing the formation of often reported impurity phases.

The change from a multiphase material to a homogeneous solid solution may be caused not only by the enhancement of the homogeneity range of the cubic phase toward the ideal ratio of the components, but also by the special nonequilibrum synthesis route. For the traditional MC synthesis route, the specimen is obtained by slowly cooling the melt to room temperature. In the cooling

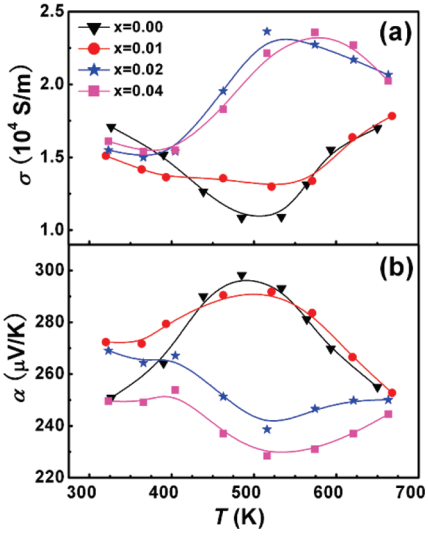

Figure 5. Temperature dependence of (a) the electrical conductivity and (b) the Seebeck coefficient of $AgSbSe_xTe_{2-x}$ ($x = 0-0.04$) samples. Lines are plotted as a guide to the eye.

process, the impurities (such as Ag_2Te) with the higher melting point solidify first and slowly grow into microscale Widmanstätten precipitates (up to ~100 μm), resulting in an inhomogeneous multiphase material. However, we use ingots that are quenched rapidly rather than slowly cooled prior to SPS processing. Rapid quenching might avoid the formation of large-scale Ag_2Te Widmanstätten precipitates in the resulting bulk material. Furthermore, due to a relatively low temperature and short SPS processing time, uniform distribution of constituents in the starting material is preserved to the maximum extent and eutectics with a lower melting point (such as $Ag_{0.35}Sb_{0.09}Te_{0.56}$) are completely suppressed.

Electrical Transport Properties. The temperature dependence of the conductivity and the Seebeck coefficient for $AgSbSe_xTe_{2-x}$ ($x = 0-0.04$) compounds is shown in Figure 5a,b. Although at ambient temperature all samples

have similar conductivities and comparable Seebeck coefficients, distinctly different trends in the temperature dependence of the electrical conductivity and the Seebeck coefficient divide the samples into two groups: those with $x = 0$ and $x = 0.01$ in one group and those with $x \geq 0.02$ in the other. With the increasing temperature, electrical conductivities of samples with $x = 0$ and $x = 0.01$ initially decrease, reach a minimum, and then increase to a value approaching the other two samples. In contrast, samples with $x \geq 0.02$ initially increase their electrical conductivity with the increasing temperature, attain maximum values near 550 K and then the nature of their transport switches back to a metallic dependence. The two very different trends result in large differences (up to a factor of 2 or more) in the magnitude of the electrical conductivity between the two groups of samples in the range 400−650 K.

As shown in Figure 5b, Seebeck coefficients of all specimens are positive reflecting the p-type form of transport. As expected, samples with high electrical conductivity have lower Seebeck coefficients and vice versa. Moreover, we observe a similar bifurcation in the behavior of the Seebeck coefficient as we have seen in the case of electrical conductivity. Samples with $x = 0$ and $x = 0.01$ have a very different temperature dependence and the magnitude of the Seebeck coefficient in comparison to samples with $x \geq 0.02$. The distinctly different trend in the transport behavior of the two groups of samples starts above 400 K (a temperature not too different from the phase transition temperature of Ag_2Te at 425 K) and is particularly amplified at temperatures near 500 K. Based on the transport behavior and the results of XRD and DSC analyses, we infer that the contrasting behavior between samples with $x = 0$ and $x = 0.01$ on one hand and those with $x \geq 0.02$ on the other is associated with the phase structure of $AgSbTe_2$. Specifically, an undoped and a weakly doped $AgSbTe_2$ ($x = 0$; 0.01) contain a complex phase structure with precipitates of Ag_2Te, whereas samples with the Se content of $x \geq 0.02$ are homogeneous solid solutions. In that context, Se-doped $AgSbTe_2$ samples reflect an intrinsic behavior of the structure, whereas the nature of transport in undoped and weakly doped $AgSbTe_2$ is influenced by the precipitated phases. At high temperatures, intrinsic excitations will dominate the transport and we expect the two groups to merge their transport behavior.

To gain more insight into the electrical transport behavior, Hall effect measurements were carried out at room temperature. The results are presented in Table 1. Unlike $AgSbTe_2$, all Se-doped samples exhibit negative Hall coefficients, contrary to the p-type character of their Seebeck coefficient. Different signs of the Seebeck and Hall coefficients are usually the sign of a multicarrier nature of transport consisting of at least one group of electrons and another group of holes.[4]

In such a two-carrier system, the Seebeck coefficient is the sum of first-order terms in the carrier mobility, as seen in eq 1

$$\alpha = \frac{\alpha_e ne\mu_e + \alpha_h pe\mu_h}{\mu_e + \mu_h} \quad (1)$$

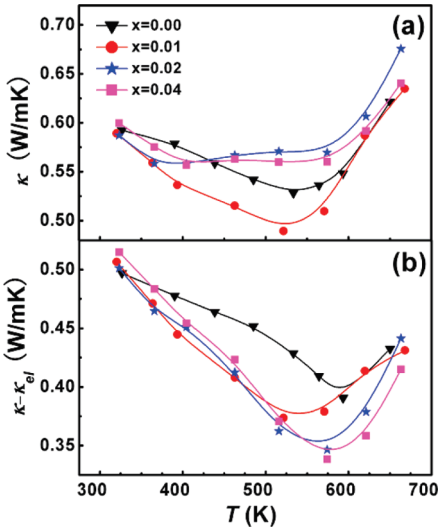

Figure 6. Temperature dependence of (a) the thermal conductivity κ and (b) the difference κ' ($= \kappa - \kappa_e$) between the total thermal conductivity and the hole contributions of $AgSbSe_xTe_{2-x}$ ($x = 0$−0.04) samples. This is not the true lattice thermal conductivity but the one augmented by the ambipolar contribution that was not subtracted from the total measured thermal conductivity. Lines are plotted as a guide to the eye.

Here, e is the charge of the carrier; p and n are the partial carrier concentrations; μ_e and μ_h are the electron and hole mobilities; and α_e and α_h are the partial electron and hole Seebeck coefficients. Therefore, the Seebeck coefficient is determined by the majority carrier. In the case of the Hall coefficient, it is the sum of quadratic terms in the carrier mobility, as given by eq 2

$$R_H = \frac{-n\mu_e^2 + p\mu_h^2}{n\mu_e + p\mu_h} \quad (2)$$

Thus, the Hall coefficient can have an opposite sign with respect to the Seebeck coefficient when the mobility of electrons is much higher than the mobility of holes. This phenomenon has been observed in $AgSbTe_2$ previously.[4] Since we deal with more than one group of carriers, we cannot deduce the concentration of holes from the Hall coefficient directly. However, the decrease in the absolute value of the Hall coefficient is related to an increase in the concentration of holes. This suggests that Se is acting as an acceptor in $AgSbTe_2$ and can optimize the hole concentration. Overall, Se doping in quantities in excess of $x = 0.02$ has a beneficial effect on the phase composition as well as electrical transport properties.

Thermal Transport Properties. Thermal conductivity as a function of temperature is shown in Figure 6a. $AgSbTe_2$ compounds are well-known for their very low thermal conductivity and our data concur. Given that thermal conductivities at and above ambient temperature are measured with no better than about 5% accuracy, it is fair to state that all samples start at 300 K with a comparable value of the thermal conductivity of close to 0.6 W/(m K). However, as the temperature increases, we observe similar bifurcation in the thermal conductivity as was seen in the behavior of the electrical conductivity and the Seebeck coefficient. Thermal conductivity of

$AgSbTe_2$ and of the sample with $x = 0.01$ initially rapidly decreases with the increasing temperature, reaches a minimum near 550 K and then turns around and increases with a further increase in temperature. Although samples with $x \geq 0.02$ also show a brief initial decrease with increasing temperature, the dependence is weaker, and above 400 K, the thermal conductivity is essentially temperature independent. This trend continues until about 600 K where the thermal conductivity starts to rise fast and both sets of samples again approach a common behavior. In the interval between 400 and 650 K, the thermal conductivity of Se doped samples with $x \geq 0.02$ is larger than the conductivity of the undoped and weakly doped ($x = 0.01$) samples.

The overall thermal conductivity κ consists of two nearly independent terms: the carrier contribution κ_{el} and a contribution due to lattice phonons, κ_{latt}. Thus, the total thermal conductivity is written as

$$\kappa = \kappa_{\text{el}} + \kappa_{\text{latt}} \quad (3)$$

Depending on the nature of transport, the electronic term may include the so-called ambipolar contribution, κ_{ambi}.[18] This contribution can be substantial in solids such as semimetals and semiconductors where both electrons and holes are present. In $AgSbTe_2$, it is estimated as being about 0.13 W/(m K) at room temperature.[4] The electronic term κ_{el} is related to the electrical conductivity via the Wiedemann–Franz law

$$\kappa_{\text{el}} = L\sigma T \quad (4)$$

where L is the Lorenz constant. We take $L = 0.7L_0$ [4] ($L_0 = \pi^2/3(k_B/e)^2 = 2.45 \times 10^{-8}\text{V}^2/\text{K}^2$ is the fully degenerate value of the Lorenz number). The lattice thermal conductivity is then obtained by subtracting both the electronic and ambipolar term from the measured total thermal conductivity. However, we do not have estimates of the partial Seebeck coefficients and the individual contributions of electrons and holes to the electrical conductivity and thus we do not know the ambipolar contribution as a function of temperature. Hence, by subtracting the electronic term from the total thermal conductivity, we obtain a lattice contribution that is inflated by the ambipolar term. This quantity is plotted in Figure 6b. In this plot, it seems that Se-doped samples with $x \geq 0.02$ have lower thermal conductivity than the undoped and a weakly doped $AgSbTe_2$. However, one must keep in mind that what is plotted in Figure 6b is not the true lattice thermal conductivity because the data are not corrected for the ambipolar contribution. Although it appears that the "lattice thermal conductivity" of Se-doped samples with $x \geq 0.02$ is lower than that of an undoped and of a weakly doped sample, conclusions whether point defects (Se substituting on the Te sites) or more extended defects such as precipitates of Ag_2Te are more effective in scattering heat-carrying phonons are not warranted. It is clear, however, that the true value of the lattice thermal conductivity of all samples in this study is very low and not too different from the theoretical minimum thermal conductivity (about 0.3 W m $^{-1}$ K^{-1}).[19]

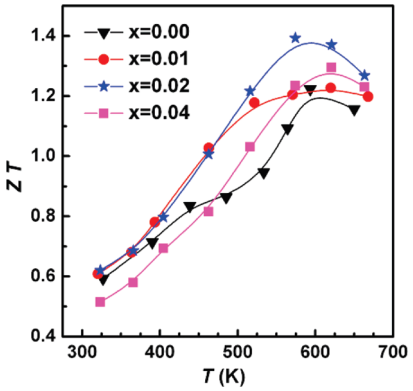

Figure 7. Temperature dependence of thermoelectric figure of merit ZT of $AgSbSe_xTe_{2-x}$ ($x = 0-0.04$) samples. Lines are plotted as a guide to the eye.

Figure of Merit *ZT*. The dimensionless thermoelectric figure of merit ZT is calculated based on the measured values of σ, α, and κ using $ZT = \alpha^2\sigma T/\kappa$. Figure 7 shows the temperature dependence of ZT of all $AgSbSe_xTe_{2-x}$ ($x = 0-0.04$) specimens. While at room temperatures the values of ZT of all samples are comparable, at elevated temperatures the benefit of Se doping is more clearly demonstrated. The highest figure of merit is observed for $AgSbSe_{0.02}Te_{1.98}$ where it reaches $ZT = 1.37$ at 565 K. This value is more than 25% higher than the figure of merit for undoped $AgSbTe_2$ at the same temperature.

Conclusion

Rather than using the traditional near-equilibrium synthesis route based on melting and slow-cooling, we prepared dense bulk p-type $AgSbSe_xTe_{2-x}$ ($x = 0-0.04$) materials by the melt-quench-spark plasma sintering process. Doping Se into the $AgSbTe_2$ matrix suppresses the often seen formation of Ag_2Te and $Ag_{0.35}Sb_{0.09}Te_{0.56}$ impurity phases and for samples with $x \geq 0.02$, the structure is a homogeneous solid solution. Different phase compositions—two-phase structures for $x = 0$ and $x = 0.01$ and a homogeneous single-phase material for $x \geq 0.02$—lead to very different behaviors in the temperature dependence of the electrical conductivity and the Seebeck coefficient. The sign of the Seebeck coefficient indicates a distinctly p-type form of transport. In contrast, room-temperature Hall effect measurements on all Se-doped samples yield a surprising negative sign. Such anomalous behavior is the consequence of two-carrier transport where the mobility of the minority carrier (electron) is much higher than the mobility of the majority holes. All compounds studied in this work are poor conductors of heat and the presence of Se in the crystal lattice of $AgSbTe_2$ leads to particularly low values of the thermal conductivity that approaches the theoretical limit for the minimum thermal conductivity. The low

(18) see, e.g., Nolas, G. S.; Sharp, J.; , Goldsmid, H. J. In *Thermoelectrics*: Springer: New York, 2001; p 44.

(19) David, G. C.; Watson, S. K.; Pohl, R. O. *Phys. Rev. B* **1992**, *46*, 6131–6140.

thermal conductivity upon doping with Se coupled with much enhanced electrical conductivity and still impressive Seebeck coefficient lead to an enhancement in the thermoelectric figure of merit that in the range between 550 and 650 K exceeds the value of $ZT = 1.35$. This value is more than 25% higher than the figure of merit of undoped $AgSbTe_2$. The results indicate that Se doping is an effective approach to synthesize homogeneous single-phase material and to enhance the thermoelectric performance of p-type $AgSbTe_2$. Further progress is likely by employing rapid solidification via melt-spinning that should result in finer nanometer-scale grain structure.

Acknowledgment. This work is sponsored by the National Basic Research Program of China (Grant 2007CB607501) and the National Science Foundation of China (Grant 50820145203 and 50731006). Research of CU at the University of Michigan is supported by a grant from the University Research Corridor.